Simultaneous Measurement of Ca^{2+} Influx and Reversal Potentials in Recombinant *N*-Methyl-D-Aspartate Receptor Channels

Ralf Schneggenburger
Ecole Normale Supérieure, Laboratoire de Neurobiologie, F-75005 Paris, France

ABSTRACT The Ca^{2+} permeability of *N*-methyl-D-aspartate receptor (NMDA-R) channels was studied in human embryonic kidney cells transfected with the NR1-NR2A subunit combination. To determine the fractional Ca^{2+} current (P_f), measurements of fura-2-based Ca^{2+} influx and whole-cell currents were made in symmetrical monovalent ion concentrations at membrane potentials between −50 mV and the reversal potential. The ratios of Ca^{2+} flux over net whole-cell charge at 2, 5, and 10 mM external Ca^{2+} concentrations ($[Ca]_o$) were identical at a membrane potential close to the reversal potential of the monovalent current component. Assuming unity of P_f at this potential, the percentage of current carried by Ca^{2+} was found to be 18.5 ± 1.3% at 2 mM $[Ca]_o$ and −50 mV. This value, which is higher than the ones reported previously, was confirmed in independent experiments in which a pure flux of Ca^{2+} through NMDA-R channels was used to calibrate the Ca^{2+} influx signals. The measured values of fractional Ca^{2+} currents, which agree with the predictions of the Goldman-Hodgkin-Katz equations, are also compatible with a two-barrier model for ion permeation, in which the differences between the energy barriers for Ca^{2+} and monovalent ions are similar on the external and internal membrane sides.

INTRODUCTION

The channels of the *N*-methyl-D-aspartate (NMDA)-type glutamate receptor are cation selective and have a high permeability for Ca^{2+}. The resulting Ca^{2+} influx through these channels is thought to be a critical step in a number of neuronal functions, including the induction of various forms of synaptic plasticity (for reviews see Bliss and Collingridge, 1993; Malenka and Nicoll, 1993). Ca^{2+} influx through NMDA-R channels has first been directly demonstrated by the use of Ca^{2+} indicator dyes in voltage-clamped spinal cord neurons (MacDermott et al., 1986; Mayer et al., 1987). To quantify the Ca^{2+} permeability of the NMDA-R channels, the attention then turned toward measurements of reversal potential shifts, which have been performed in cultured neurons (Mayer and Westbrook, 1987; Ascher and Nowak, 1988; Iino et al., 1990; Jahr and Stevens, 1993; Zarei and Dani, 1994) as well as in neurons in brain slices (Spruston et al., 1995; Koh et al., 1995) and in recombinant NMDA-R channels (Burnashev et al., 1992, 1995). In most of this work, the Ca^{2+}-induced reversal potential shifts were interpreted using the Goldman-Hodgkin-Katz (GHK) voltage equations extended for the use of divalent cations (Jan and Jan, 1976; Lewis, 1979). The resulting permeability ratio of Ca^{2+} with respect to various monovalent cations, such as Na^+, K^+, and Cs^+ (P_{Ca}/P_M), was found to be in the range of 3 to 5 (when no corrections for ionic activities were made). It is thus generally accepted that the NMDA-R channel has a relatively high permeability for Ca^{2+} with respect to monovalent cations.

To deduce from the permeability ratio P_{Ca}/P_{mono} the percentage of current carried by Ca^{2+} (also called the "fractional Ca^{2+} current" or P_f; Schneggenburger et al., 1993) at negative membrane potentials, a model for ion permeation has to be assumed. In the simplest case, the ion permeation process could be modeled with an energy barrier model in which the barrier heights for Ca^{2+} have a constant offset from the barrier heights for monovalent ions (i.e., the "constant offset energy peak condition" is met; see, e.g., Lewis and Stevens, 1979; Hille, 1992). The P_f value predicted by such a model is quite similar to the value predicted by the GHK equations and is around 17% for an NMDA-R channel with a P_{Ca}/P_M of 4 (Mayer and Westbrook, 1987), when considering a membrane potential of −50 mV and an external Ca^{2+}-concentration ($[Ca]_o$) of 2 mM. However, there is no direct evidence to date that the constant offset energy peak condition indeed holds for NMDA-R channels, and slight asymmetric variations of the relative barrier height for Ca^{2+} over monovalent cations can produce significant deviations of P_f at negative membrane potentials.

Recently, methods have been devised that allow a direct, model-independent measurement of the fractional Ca^{2+} current (Schneggenburger et al., 1993; Zhou and Neher, 1993; Vernino et al., 1994; see Neher, 1995, for a review). With this approach, which employs combined whole-cell current- and fura-2-based Ca^{2+} influx measurements, an estimation of the fractional Ca^{2+} current through NMDA-R channels in septal neurons was given with 7%, at a $[Ca]_o$ of 1.6 mM and a membrane potential of −80 mV (Schneggenburger et al., 1993). More recently, using a $[Ca]_o$ of 1.8 mM, a P_f value of 11% at −60 mV has been reported for recombinant NMDA-R channels composed of the NR1-NR2A subunits expressed in human embryonic kidney (HEK) cells (Burnashev et al., 1995). The values reported in both studies are

Received for publication 4 December 1995 and in final form 26 January 1996.

Address reprint requests to Dr. Ralf Schneggenburger, Ecole Normale Supérieure, Laboratoire de Neurobiologie, 46, rue d'Ulm, F-75005 Paris, France. Tel.: ++33-1-4432-3752; Fax: ++33-1-4432-3887; E-mail: rschneg@wotan.ens.fr.

0006-3495/96/05/2165/10 $2.00

smaller than the value of about 17%, which is predicted by simple models of ion permeation (see above) for the native NMDA-R channel under similar ionic conditions.

Because of the pivotal functional role of Ca^{2+} entry through neuronal NMDA-R channels, it was desirable to understand the reason for the difference between measured P_f values and P_f values predicted by the GHK equation from permeability ratios. Therefore, NMDA-induced whole-cell currents and Ca^{2+} influx signals were measured in HEK cells transfected with either the NR1-NR2A or the NR1-NR2B subunit combination. Two different approaches were used for the estimation of P_f values. In the first method, Ca^{2+} influx signals and whole-cell currents were measured in the presence of internal and external permeant monovalent cations, both at negative membrane potentials (−50, −30 mV) and at membrane potentials just negative to the reversal potential. P_f should approach unity, or 100%, at the reversal potential of the monovalent current component, a fact that was used to calibrate the fura-2-based Ca^{2+} influx signals and to calculate the P_f values over an extended range of membrane potentials. Surprisingly, it became apparent that P_f at two different values of $[Ca]_o$ (2 and 10 mM) was in rather good agreement with the prediction made by the GHK equation, with a value of around 18% at 2 mM $[Ca]_o$ and −50 mV. This value was confirmed in measurements using the second approach for estimating P_f, in which ion substitution experiments were used to create a pure flux of Ca^{2+} through the NMDA-R channel (see Vernino et al., 1994) to calibrate the Ca^{2+} influx measurements.

MATERIALS AND METHODS

Expression of NMDA-R subunits and electrophysiological recordings

Transient transfection of human embryonic kidney (HEK) cells with the NMDA-R subunits NR1-NR2A (or NR1-NR2B in some cases) was done with the calcium phosphate precipitation method, using a DNA ratio of 1 (NR1):3 (NR2-subunits), at a total amount of 2 μg of plasmid DNA/35-mm culture dish. HEK cells were kept in cell culture according to standard procedures. About 8 h before transfection, cells were plated on poly-L-lysine-coated coverslips at a density intended to yield a high number of single cells. The cells were kept in a glutamate and aspartate-free medium, which was supplemented with 200 μM of the NMDA-R antagonist D-L APV after transfection. The NMDA-R subunit clones were gifts from the laboratories of Drs. S. Nakanishi (NR1; Moriyoshi et al., 1991, identical to the splice variant NR1–1a in the nomenclature of Hollmann et al., 1993) and P. Seeburg (NR2A, NR2B; Monyer et al., 1992) and were subcloned into a mammalian expression vector (pcDNA3; Invitrogene, Leek, The Netherlands).

Cells were used for recording 12–36 h after transfection. To screen for cells expressing NMDA-R channels, the cells were briefly (5 min) loaded with the membrane-permeable Ca^{2+} indicator fura-2 AM, using a concentration of 0.5 μM in the bathing medium. Cells that responded to short (2-s) pulses of 50–100 μM NMDA with a transient elevation of intracellular Ca^{2+} were selected for the experiments and regularly showed NMDA-induced inward currents. At a later stage, coexpression of the fluorescent expression marker green fluorescent protein (GFP) (Marshall et al., 1995; the GFP containing plasmid DNA was a gift of D. Pritchett) was used for screening transfected cells. The amplitude of the cellular GFP fluorescence at an excitation light of 380 nm was in the range of 0.1–0.3 bead units (BU; see below for definition). Thus, the GFP fluorescence at 380-nm excitation wavelength represented a background signal for the fura-2-based Ca^{2+} influx measurements. However, the GFP background signal should not have influenced the estimation of P_f, because it was found not to be changed by Ca^{2+} influx through NMDA-R channels (n = 3 cells, which were recorded without Ca^{2+} buffers added to the pipette solution). The GFP background signal was small compared to the fluorescence signal at 380 nm of HEK cells completely loaded with 1 mM fura-2, which was in the range of 2–4 BU.

Whole-cell patch-clamp recordings (Hamill et al., 1981) were made using pipette solutions based on 140 mM CsCl, 10 mM HEPES (pH 7.2 for all intracellular solutions). This solution was complemented with 5 μM Cs_2-EGTA for the measurements of reversal potential changes (see Fig. 1) or with 1 mM K_5-fura-2, 4 mM Na_2-ATP, 4 mM $MgCl_2$ for measuring Ca^{2+} influx signals. The extracellular solution contained (in mM) 150 NaCl, 0.1 glycine, 10 HEPES (pH 7.4 by adding NaOH). $CaCl_2$ was added from a stock solution of 1 M to give external Ca^{2+} concentrations ($[Ca]_o$) of 0.1–10 mM. In some experiments, the intracellular CsCl and the external NaCl were replaced by 150 mM *N*-methyl-D-glucamine Cl (NMG) (Fig. 4).

Patch-pipettes had resistances of 2–3 MΩ when filled with the CsCl-containing pipette solutions, and the access resistance was 6.3 ± 1.7 MΩ (n = 19). Single and preferentially small HEK cells (cell capacitance of 10.8 ± 4.2 pF, n = 19) were chosen for recordings to allow a fast fura-2 loading, good voltage control, and a fast and uniform exchange of extracellular solutions. Recordings were made from cells attached to the bottom of the recording chamber to avoid movement artefacts in the fura-2 recordings. During recording, the cells were continuously perfused from a nearby outlet tube (inner diameter of around 0.4 mm), and agonist applications (NMDA, 10–100 μM) were made in the continuous presence of 100 μM glycine with a valve-controlled perfusion system similar to the ones described by Konnerth et al. (1987) and Lin and Stevens (1994). Membrane currents were recorded with an EPC-7 patch-clamp amplifier (List electronics, Darmstadt, Germany), low-pass filtered at 3 kHz, and then sampled in sweeps of 2048 points using data acquisition software (Pclamp6; Axon Instruments, Foster City, CA). All chemicals were obtained from Sigma (Paris, France), except for fura-2 AM and fura-2 pentapotassium salt (Molecular Probes, Eugene, OR). Experiments were performed at room temperature (20–22°C). Average results were given as mean values ± standard deviation.

Fura-2-based measurements of Ca^{2+} influx

The Ca^{2+} influx was measured directly from the change in the Ca^{2+}-sensitive fura-2 fluorescence at 380-nm excitation light (F_{380}), as previously described (Neher and Augustine, 1992, and other studies; for a review see Neher, 1995). An inverted microscope equipped for epifluorescence was used with a 40×, 0.75 NA water immersion objective (Zeiss, Oberkochen, Germany), and a filter wheel rotating at 4 Hz produced alternating excitation of fura-2 at 360-nm and 380-nm wavelength. Fluorescence was measured with a photomultiplier tube, which received its light input from a circular area of about 30 μm diameter. To account for variations in excitation light intensity or detection efficiency, which can occur between different experiments, the F_{380} signals were divided by the average fluorescence at 380 nm of n = 5 beads (diameter 4.5 μm; Polysciences, Warrington, PA) measured after the experiment. By this procedure, the F_{380} signals are given in "bead units" (abbreviated 1 BU; see Zhou and Neher, 1993; Schneggenburger et al., 1993).

The background-corrected fluorescence ratio, F_{360}/F_{380}, was used to calculate the intracellular free Ca^{2+} concentration ($[Ca]_i$) using the formula given by Grynkiewicz et al. (1985). The calibration parameters of the set-up were determined in whole-cell recordings from HEK cells by controlling $[Ca]_i$ with mixtures of $CaCl_2$ and EGTA, assuming a dissociation constant of 150 nM for the Ca^{2+}-EGTA complex under these conditions.

Ca^{2+} influx measurements were performed after equilibration of the fura-2 concentration between the pipette and the cell, which was nearly complete after 2–4 min of whole-cell recording. Only NMDA currents

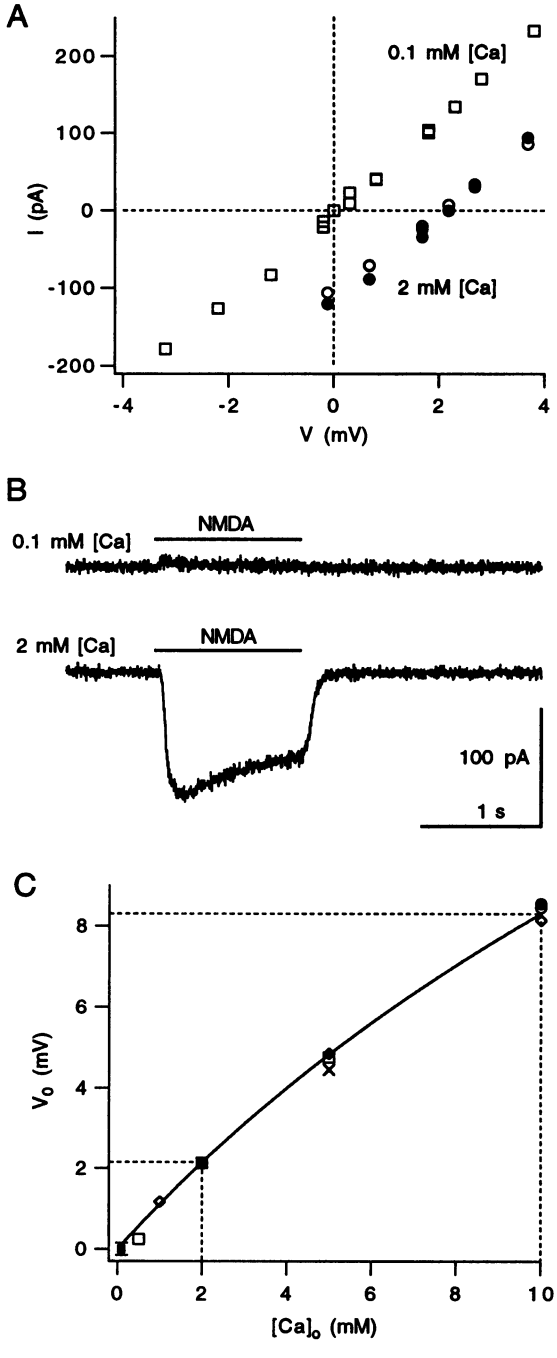

FIGURE 1 Reversal potential shifts induced by changing $[Ca]_o$ in NMDA-R channels composed of NR1-NR2A subunits. (*A*) Current-voltage relationships constructed from peak current amplitudes of whole-cell responses to 100 μM NMDA at 2 mM $[Ca]_o$ (*closed* and *open symbols* are for control and recovery, respectively) and at 0.1 mM $[Ca]_o$ (*open squares*). The membrane potential (V) was given relative to $V_{0,M}$ (see Materials and Methods). (*B*) Two traces from the same cell as shown in *A*, recorded subsequently at the same membrane potential (V = 0 mV). Note the NMDA-induced inward current after changing $[Ca]_o$ to 2 mM. NMDA applications are indicated by horizontal bars. (*C*) Reversal potential shift as a function of $[Ca]_o$ in the range of 0.1–10 mM (n = 11 cells). The line represents the fit of the extended GHK voltage equation (Eq. 5) to the data, with P_{Ca}/P_M = 3.6 (without correcting for ionic activities; see Materials and Methods). The fit predicts that the reversal potential in the absence of external Ca^{2+} ($V_{0,0Ca}$) is 2.1 mV and 8.3 mV negative to the reversal potentials in 2 and 10 mM $[Ca]_o$, respectively.

leading to peak $[Ca]_i$ values of less than 200 nM were considered in the analysis, because the effective Ca^{2+}-sensitive fluorescence change is expected to drop to smaller values when a significant amount of fura-2 is in the Ca^{2+}-bound form (Neher and Augustine, 1992). It is assumed that in these conditions, i.e., at 1 mM fura-2 and $[Ca]_i \leq 200$ nM, fura-2 is the main Ca^{2+} buffer and is binding virtually all of the incoming Ca^{2+}, as has been shown in bovine chromaffin cells (Neher and Augustine, 1992) and in HEK cells (Burnashev et al., 1995). However, the value of the estimated fractional Ca^{2+} current should be independent of this assumption as long as Ca^{2+} influx signals are compared between similar Ca^{2+} buffering conditions.

To quantify the fraction of Ca^{2+} contributing to the NMDA-induced currents, the ratio of F_{380} over the net whole-cell charge (the "FQ ratio"; see Schneggenburger et al., 1993) was determined:

$$FQ = \frac{\Delta F_{380}}{\int I\,dt}. \quad (1)$$

This ratio has the dimension of fluorescence intensity/electrical charge, i.e., BU/nC. The FQ ratio was obtained by calculating the time integral of the leak-subtracted current response, which was then multiplied by a scaling factor (FQ) to fit the integrated current to the F_{380} signal (see Figs. 2 and 4).

By dividing the FQ ratio by a reference FQ ratio obtained under experimental conditions in which the net NMDA-activated current is expected to be carried exclusively by Ca^{2+} (see below and Results), the fractional Ca^{2+} current (P_f) can be obtained. The P_f values are given as percentage values.

Measurements of reversal potential shifts

The reference electrode was an Ag/AgCl electrode inside an agar bridge filled with external solution (150 mM NaCl, 10 mM HEPES, 2 mM $CaCl_2$). By changing $[Ca]_o$ from 0 to 10 mM in the external solution, a liquid junction potential shift of +0.6 mV was detected using the agar bridge reference electrode and a second, streaming 3 M KCl electrode, as described by Neher (1992). Although this liquid junction potential was relatively small compared to the reversal potential shift of the NMDA current for the same change in $[Ca]_o$ (around +8 mV; see Fig. 1 *C*), a correction for the liquid junction potential was made at each $[Ca]_o$, assuming that a linear relation exists between the liquid junction potential shift and $[Ca]_o$.

The first method used for determining the reference FQ ratio required the knowledge of the reversal potential of the monovalent current component ($V_{0,M}$) of the total NMDA-induced current in the presence of external Ca^{2+}. To determine $V_{0,M}$ it was assumed that $V_{0,M}$ is equal to V_0 in the absence of external Ca^{2+} ($V_{0,0Ca}$). The value of $V_{0,0Ca}$ can, in principle, be obtained for every cell in which fura-2-based Ca^{2+} influx measurements are made. However, holding the cells in a solution with low $[Ca]_o$ (0.1 mM) often led to an irreversible degradation of the seal resistance. Therefore, $V_{0,0Ca}$ was estimated relative to the reversal potential at 2 mM $[Ca]_o$ ($V_{0,2Ca}$) in a limited number of cells by changing $[Ca]_o$ from 2 mM to 0.1 mM and back to 2 mM (see Fig. 1, *A* and *B*). The average value of this reversal potential shift was found to be -2.13 ± 0.15 mV (n = 5 cells) after correcting for a liquid junction potential shift, which was estimated to be -0.12 mV for the corresponding change in $[Ca]_o$ (see above).

Reversal potential shifts were measured in similar experiments in a range of $[Ca]_o$ of up to 10 mM. The data (n = 11 cells; Fig. 1 *C*) were fitted with the extended GHK voltage equation (Eq. 5), giving a permeability ratio of P_{Ca}/P_M = 3.6 (without correcting for ionic activities; see below). Eq. 5 predicts, at P_{Ca}/P_M = 3.6, that $V_{0,0Ca}$ is -2.1 mV negative from $V_{0,2Ca}$ and -8.3 mV negative from $V_{0,10Ca}$.

In the experiments in which P_f was measured in the presence of permeant monovalent ions and at 2 or 10 mM $[Ca]_o$ (see Figs. 2, 3), $V_{0,M}$

was therefore calculated from the measured values of $V_{0,2Ca}$ and $V_{0,10Ca}$ according to

$$V_{0,M} = V_{0,2Ca} - 2.1\ mV - V_{LJ(Ca)}$$

and

$$V_{0,M} = V_{0,10Ca} - 8.3\ mV - V_{LJ(Ca)}. \quad (2)$$

Here, $V_{LJ(Ca)}$ is the (small) liquid junction potential change induced by adding $CaCl_2$ to the external solution (see above). $V_{0,M}$ was -1.4 ± 1.3 mV ($n = 8$ cells at 2 mM $[Ca]_o$). Because $V_{0,M}$ was close to 0 mV but varied slightly between different experiments, the membrane potential (V) was given relative to $V_{0,M}$:

$$V = V_h - V_{0,M}. \quad (3)$$

V_h refers to the voltage reading on the patch-clamp ampifier.

Simulations of fractional Ca^{2+} currents

The basic assumption underlying the permeation models for calculating fractional Ca^{2+} currents was that $P_f = 100\%$ at $V_{0,M}$, independent of $[Ca]_o$. This assumption, which is implicit in the GHK equations where ions obey the independence principle (see Hille, 1992), may also hold in other cases. In particular, if a one-ion channel is considered in which either a Ca^{2+} or a monovalent ion binds inside the pore at a given time, the independence principle might be violated at large driving forces and high permeant ion concentrations, and yet, provided the permeation of monovalent ions is "normal" during the period when Ca^{2+} ions are not bound, the value of the reversal potential of the monovalent current component will not change with $[Ca]_o$.

To calculate P_f, two simple models were used that both obey the above assumption. In the first, P_f is derived (Eq. 4) from the GHK current equations (Schneggenburger et al., 1993), assuming 1) that $[Ca]_i$ is negligible (it was $\leq$200 nM in these measurements; see above) and 2) that the permeability of monovalent ions (P_M) is the same for Cs^+ and Na^+. The last assumption has been made before for the NMDA-R channel (Mayer and Westbrook, 1987), and it seems justified here because $V_{0,M}$ was found to be close to 0 mV in the virtually symmetrical monovalent ion conditions employed here (see above).

$$P_f = \frac{[Ca]_o}{[Ca]_o + \frac{P_M}{P_{Ca}} * \frac{[M]}{4} * \left(1 - \exp\left(2V\frac{F}{RT}\right)\right)}. \quad (4)$$

Here, V is the membrane potential; F, R, and T have their usual meaning; [M] is the monovalent ion concentration (155 mM); $[Ca]_o$ is the extracellular free Ca^{2+} concentration; and P_M/P_{Ca} is the permeability ratio of monovalent over Ca^{2+} ions. From this equation, it can be seen that at $V =$ 0 mV (corresponding to $V_{0,M}$), $P_f = 1$, or 100%, at any given $[Ca]_o$, as predicted by the principle of independence of ionic movement.

P_{Ca}/P_M was obtained by fitting the extended GHK voltage equation to the reversal potential shift induced by changing $[Ca]_o$ in the range of 0.1–10 mM (see Fig. 1 *C*). Under the assumptions outlined above for the derivation of Eq. 4, the extended GHK voltage equation given by Jan and Jan (1976) simplifies to

$$V_0 = \frac{RT}{F} * \ln \frac{\left(4[M]\left([M] + 4\frac{P_{Ca}}{P_M}[Ca]_o\right)\right)^{1/2}}{2[M]}. \quad (5)$$

P_{Ca}/P_M was varied as the free parameter to fit the data shown in Fig. 1 *C*, using the user-defined fit function of a data analysis program (IgorPro, Wavemetrics, OR).

Values for $[Ca]_o$ are given as concentrations rather than ionic activities, because P_f values can be directly related to Ca^{2+} concentrations. Therefore, the value of $P_{Ca}/P_M = 3.6$ used in Eqs. 4 and 5 and referred to in the text was not corrected for ionic activities. For simulating P_f using the energy barrier model (see below), activity coefficients of 0.5 for Ca^{2+} in the concentration range of 0.1 to 10 mM and 0.71 for the monovalent cations were used (see also Jahr and Stevens, 1993; Spruston et al., 1995). With these activity coefficients, $P_{Ca}/P_M = 5.1$ for the data shown in Fig. 1 *C*.

In the second model, P_f was simulated using a symmetrical one-site, two-barrier model based on Eyring rate theory. The electrical distance of the ion binding site through the field was arbitrarily set to 0.5. The isolated current components of a monovalent current (I_M, assuming, as above, that $P_{Na} = P_{Cs} = P_M$) and a Ca^{2+} current (I_{Ca}, activity coefficients as above) were calculated from the voltage-dependent rate constants as described by Lewis and Stevens (1979). P_f was calculated as (see Schneggenburger et al., 1993)

$$P_f = \frac{I_{Ca}}{I_{Ca} + I_M}.$$

A good fit of the data was obtained if it was assumed that the constant offset energy peak condition is met, i.e., that the difference in barrier heights for monovalent and Ca^{2+} ions is the same for all barriers (see Hille, 1992, for review). In this case, the difference in barrier height ($\Delta\Delta G$) for Ca^{2+} and monovalent ions is directly related to P_{Ca}/P_M:

$$\Delta\Delta G = \ln P_{Ca}/P_M$$

For $P_{Ca}/P_M = 5.1$ (after correction for ionic activities), which was obtained from the fit of Eq. 5 to the data in Fig. 1 *C*, $\Delta\Delta G = 1.63\ RT$ units at 0 mV. As expected, the prediction of P_f using this value of $\Delta\Delta G$ was the same as the GHK prediction for P_f at membrane potentials close to V_0 (see Fig. 3). The prediction of P_f was independent of the well depths and of the absolute heights of the barriers for Ca^{2+} or monovalent ions.

RESULTS

To determine the fractional Ca^{2+} current (P_f) through NMDA-R channels composed of NR1-NR2A subunits, Ca^{2+} fluxes were measured as the change in the Ca^{2+}-sensitive fluorescence at 380-nm excitation (F_{380}) using saturating intracellular fura-2 concentrations (1 mM; see Neher, 1995). The quantity FQ ratio was derived by dividing the fluorescence change ΔF_{380} by the simultaneously recorded whole-cell charge. A reference FQ ratio for calculating P_f was obtained in every cell in which measurements of P_f were made. This was done in two different experimental approaches, in which P_f was measured either in the presence or in the absence of internal permeant monovalent cations.

Fractional Ca^{2+} currents in the presence of internal permeant monovalent cations

In the first approach to measuring P_f, Ca^{2+} influx measurements were made in the presence of internal and external permeant monovalent cations. The reference FQ ratio for calculating P_f values was obtained at the reversal potential of the monovalent current component of the NMDA response. This reversal potential ($V_{0,M}$) was evaluated as explained in the following.

Measurements of the reversal potential shift induced by varying $[Ca]_o$ in a range of 0.1 to 10 mM were made at

constant external [Na] in a first series of experiments (see Fig. 1; see also Mayer and Westbrook, 1987). The plot of reversal potential shifts versus $[Ca]_o$ was fitted with the extended GHK voltage equation (Eq. 5). An extrapolation of this fit to 0 $[Ca]_o$ indicates the reversal potential in the absence of external Ca^{2+} ($V_{0,0Ca}$). In addition, the fit of the extended GHK equation to the data in Fig. 1 *C* indicated a permeability ratio, P_{Ca}/P_M, of 3.6.

For calculating the reversal potential of the monovalent current component in the presence of external Ca^{2+} ($V_{0,M}$) from the average data in Fig. 1, an important assumption was made: it was assumed that $V_{0,0Ca}$ does not change by adding external Ca^{2+}, as is predicted by the principle of independence of ionic movement (see Hille, 1992). $V_{0,M}$ can then be calculated relative to the measured reversal potentials at 2 or 10 mM [Ca]o (see Eq. 2 in Materials and Methods). At $V_{0,M}$, the net inward current in the presence of external Ca^{2+} represents a pure flux of Ca^{2+}, and thus P_f = 100%. The *FQ* ratio at $V_{0,M}$ can therefore be used to obtain a reference *FQ* ratio for calculating P_f.

Whole-cell recordings and simultaneous Ca^{2+} influx measurements were then made for NMDA-R channels composed of the NR1-NR2A subunit combination at 2 mM $[Ca]_o$. In the example of Fig. 2 *A*, during an NMDA (100 μM) application of 1.2 s at −50 mV, a charge accumulation of roughly −450 pC occurred, as can be seen from the time integral of the current response (Fig. 2 *A, top, thin line*). When the time integral was superimposed on the F_{380} trace and multiplied with the corresponding *FQ* ratio, a good fit of the time course of F_{380} was obtained. This is indeed expected for a Ca^{2+} influx, which is short in comparison to the time course of $[Ca]_i$ recovery (Schneggenburger et al., 1993). The time constant of $[Ca]_i$ recovery, when fitted with a single exponential function, was found to be 35.4 ± 13 s in these experiments (n = 9 cells, V_h = −50 mV).

After determining the *FQ* ratios at negative membrane potentials (−50, −30 mV), whole-cell currents and Ca^{2+} influx signals were analyzed in particular detail close to the reversal potential. Fig. 2 *B* shows the whole-cell current and the associated Ca^{2+} influx close (+0.1 mV) to the calculated reversal potential of the monovalent current component ($V_{0,M}$). Although the amplitude of the whole-cell current was small, the time integral of the current response, when multiplied by an *FQ* ratio of 7.5 BU/nC in this example, gave a reliable fit of the measured change in F_{380} (Fig. 2 *B, bottom*). Here, the duration of the NMDA application was doubled with respect to the example shown in Fig. 2 *A*, to compensate for the smaller total influx of Ca^{2+} at the more positive membrane potential (compare the slopes of F_{380} in Fig. 2, *A* and *B*).

Measurements of *FQ* ratios at 2 mM $[Ca]_o$ at membrane potentials between −50 mV and the reversal potential of the current responses were made in eight cells. A linear interpolation between the *FQ* ratios closest to $V_{0,M}$ gave a reference *FQ* ratio for every cell, which was used to calculate the P_f values at all examined membrane potentials. The resulting average P_f values are shown in Fig. 3 (n = 8 cells, *closed symbols*). In this analysis, P_f was found to be 18.5 ± 1.3% at −50 mV.

To obtain an estimate of P_f through NMDA-R channels at an elevated $[Ca]_o$, a similar series of experiments as described above for 2 mM $[Ca]_o$ was performed at 10 mM $[Ca]_o$. At this $[Ca]_o$, the P_f at −50 mV is expected to be about 50%, and thus, NMDA applications might cause a large influx of Ca^{2+}. To avoid binding of a significant amount of fura-2 to Ca^{2+}, which would lead to an underestimation of the Ca^{2+}-sensitive fluorescence signal (see Neher and Augustine, 1992), special care was taken to limit the peak $[Ca]_i$ values to less than 200 nM. This was done by reducing the duration of the agonist application (to a minimum of 0.6 s) or by applying lower concentrations of NMDA (10 or 30 μM) when necessary. The reference *FQ* ratio was obtained by linear interpolation to the value at $V_{0,M}$ and was used to calculate the P_f values at all membrane

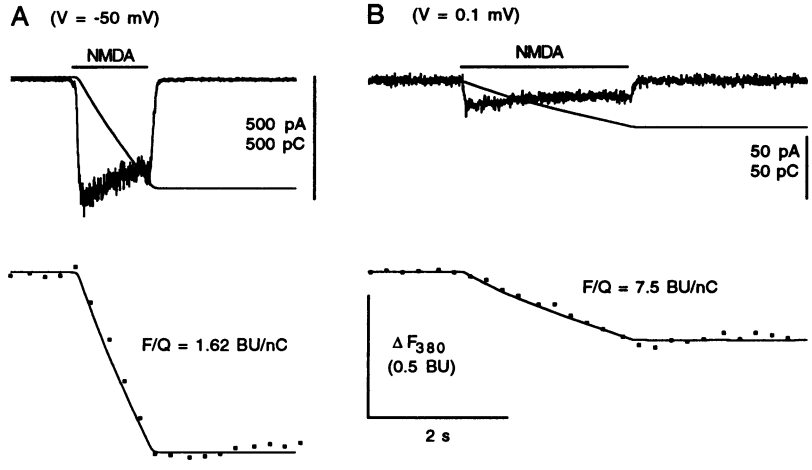

FIGURE 2 Measurements of whole-cell currents and Ca^{2+} influx at different membrane potentials. (*A, B*) NMDA (100 μM)-induced whole-cell currents (*top*) and Ca^{2+}-sensitive fluorescence changes (ΔF_{380}, *bottom*) at 2 mM $[Ca]_o$ at −50 mV (*A*) and at 2 mV negative to the observed reversal potential (V = 0.1 mV) (*B*). The time integral of the leak-subtracted current is shown as a thin line (*top*). After multiplication with the respective *FQ* ratios, the current integrals fit well the time courses and amplitudes of the F_{380} signals (*bottom*). Note that the current scaling is changed in *B* with respect to *A*.

potentials studied (see Fig. 3, *open symbols*), revealing a value of 55 ± 4% (n = 3 cells) at −50 mV.

In the plot of Fig. 3, the predictions of P_f from the GHK equation and the symmetrical barrier model are superimposed on the data (*solid* and *dashed lines*, respectively; a P_{Ca}/P_M of 3.6 was used in both models; see Materials and Methods). As can be seen, the P_f values are in reasonable agreement with the model predictions over a wide voltage range, with a slight tendency of deviation toward larger P_f values at negative membrane potentials.

Table 1 lists the reference FQ ratios found by linear interpolation of the values close to $V_{0,M}$. In a subset of cells (n = 3) in which FQ ratios were measured at 2 mM $[Ca]_o$, an estimation of the reference FQ ratio was also obtained at 5 mM $[Ca]_o$. As can be seen, similar values for the reference FQ ratio were obtained at three different $[Ca]_o$ values.

Fractional Ca^{2+} current in the absence of internal permeant monovalent ions

Because the method for calculating P_f values in the experiments with internal and external permeant monovalent cations depends on the assumption that P_f is unity at $V_{0,M}$, it was desirable to obtain an estimation of P_f using a different method for calibrating the FQ ratios. By using impermeant monovalent cations in the internal and external solutions and elevated $[Ca]_o$, a whole-cell current can be induced by NMDA application, which represents a pure flux

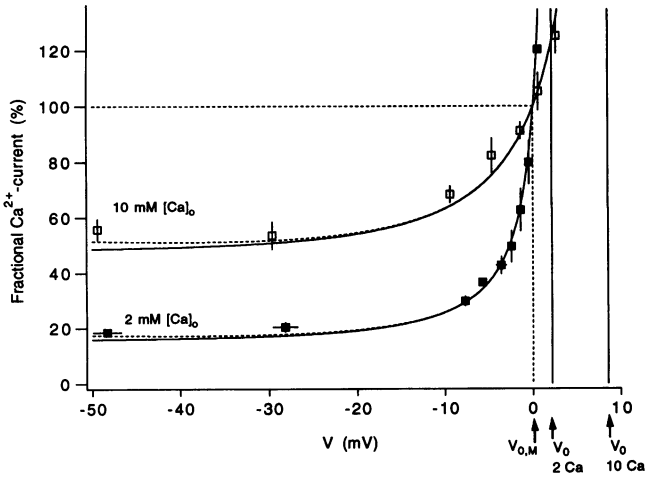

FIGURE 3 Fractional Ca^{2+} currents through NMDA-R channels at 2 and 10 mM $[Ca]_o$ as a function of membrane potential, in the presence of internal and external permeant monovalent cations. The membrane potential (V) is given relative to $V_{0,M}$. The observed reversal potentials at 2 or 10 mM $[Ca]_o$ are indicated by arrows. P_f was calculated using the reference FQ ratio obtained at $V_{0,M}$. Data were averaged in voltage groups (n = 8 cells at 2 mM $[Ca]_o$, n = 3 cells at 10 mM $[Ca]_o$). Standard deviations larger than the symbol size were added to the plot, except for the value at 2 mM $[Ca]_o$, +0.4 mV (SD = ±18%), which was omitted for clarity. Simulations of P_f based on the GHK current equations (Eq. 4, *solid line*, P_{Ca}/P_M = 3.6) and on a symmetrical one-site, two-barrier model (*dashed line*, P_{Ca}/P_M = 3.6, see Materials and Methods) are superimposed on the data.

TABLE 1 Reference *FQ* ratios estimated in various ionic conditions

External ionic concentrations (in mM)	*FQ* ratio (BU/nC)
2 Ca, 155 Na*	8.0 ± 0.6 (8)
5 Ca, 155 Na*	8.1 ± 0.2 (3)
10 Ca, 155 Na*	7.9 ± 0.2 (3)
10 Ca, 150 NMG‡	10.4 ± 0.8 (14)

*FQ ratios estimated at $V_{0,M}$ with the Cs-containing internal solution.
‡FQ ratios at −50 mV with the NMG-containing internal solution.

of Ca^{2+} through the NMDA-R channels. By subsequently switching the external solution to a mixture of Ca^{2+} and Na^+, the fractional contribution of Ca^{2+} to the unidirectional flux of both cations can be determined by comparing the FQ ratios obtained in both experimental conditions, an approach similar to the one used previously by Vernino et al. (1994).

Internal and external permeant cations were replaced by 150 mM NMG, which in NMDA-R channels is virtually impermeant ($P_{NMG}/P_{Cs} \leq 0.01$ in NR1-2A channels; Villarroel et al., 1995), and 10 mM $CaCl_2$ was added to the external solution. Example traces of NMDA-induced membrane currents and F_{380} signals under these experimental conditions are shown in Fig. 4 *A*. The FQ ratio in this example was 10.8 BU/nC and was found to be 10.4 ± 0.8 BU/nC (n = 14 cells) on average. As expected for the case of a pure influx of Ca^{2+}, the measured FQ-ratios were independent of the membrane voltage (−50 to +5 mV, n = 7 cells; see Fig. 4 *C*). Furthermore, when $[Ca]_o$ was reduced from 10 mM to 0.1 mM, a reduction of the NMDA-induced inward currents by more than 90% was observed (n = 4 cells; not shown). This suggests that the observed inward currents indeed represented a pure influx of Ca^{2+}, despite the presence of 5 mM K^+ after adding 1 mM fura-2 pentapotassium salt to the internal solution.

In Fig. 4 *B*, the effects of changing the ionic composition of the external solution to 155 mM Na^+, 2 mM Ca^{2+} on the whole-cell currents and Ca^{2+} influx signals are shown for the same cell, as illustrated in Fig. 4 *A*. The FQ ratio was 1.6 BU/nC in this example. By dividing this value by the reference FQ ratio obtained in the same cell in the presence of 150 mM NMG^+, 10 mM Ca^{2+}, a P_f value of 14.8% was obtained. On average, P_f was found to be 16.0 ± 1.2% (n = 8 cells; see *right bar* in Fig. 5) when this approach was used.

The bar graph in Fig. 5 summarizes the P_f values obtained in the different experimental conditions at a membrane potential of −50 mV. The values of P_f predicted by the symmetrical barrier model (see Materials and Methods; P_{Ca}/P_M of 3.6) are indicated by horizontal arrowheads. The value at 2 mM $[Ca]_o$ in the presence of internal Cs^+ (P_f = 18.5 ± 1.3%; Fig. 5, *middle bar*) is larger than the value found at 2 mM $[Ca]_o$ in the absence of internal permeant cations (P_f = 16.0 ± 1.2%; Fig. 5, *right bar*), as expected from the fact that at −50 mV the Na^+-inward current is partly counterbalanced by a Cs^+ outward current component.

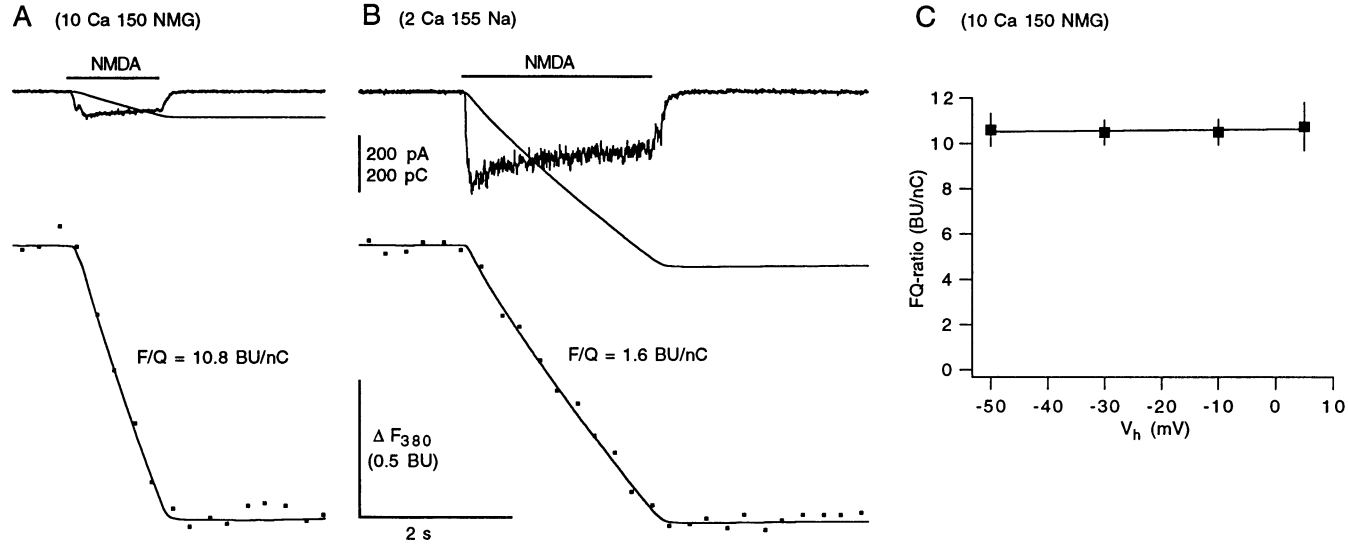

FIGURE 4 Measurement of fractional Ca^{2+} currents through NMDA-R channels in the absence of internal permeant monovalent cations. The internal solution contained 150 mM NMG^+ as the main cation. (*A*) In an external solution containing 10 mM Ca^{2+}, 150 mM NMG^+, an *FQ* ratio of 10.8 BU/nC was observed in this example. (*B*) After changing to an external solution containing 155 mM Na^+, 2 mM Ca^{2+}, an *FQ* ratio of 1.6 BU/nC was observed. $V_h = -50$ mV, same scales for *A* and *B*. (*C*) The *FQ* ratios in the presence of 10 mM $[Ca]_o$, 150 mM NMG^+ as a function of membrane potential. Averaged values of $n = 7$ cells are plotted. The line is a linear regression to the data points.

The Ca^{2+} permeability of NMDA-R channels composed of the NR1-NR2B subunit combination

In many brain regions, the NR1 subunit forms heteromeric channels with either the NR2A or with the NR2B subunit (Monyer et al., 1992; Watanabe et al., 1992; Monyer et al., 1994). To obtain an estimate of the Ca^{2+} permeability of NMDA-R channels assembled with NR2B subunits, reversal potential shifts were measured in HEK cells expressing the NR1-NR2B subunit combination. The reversal potential shift induced by changing $[Ca]_o$ from 2 to 10 mM was $+6.24 \pm 0.48$ mV ($n = 4$ cells), which is similar to the one observed (see Fig. 1 *C*) for the NR1-NR2A subunit combination for the same change in $[Ca]_o$.

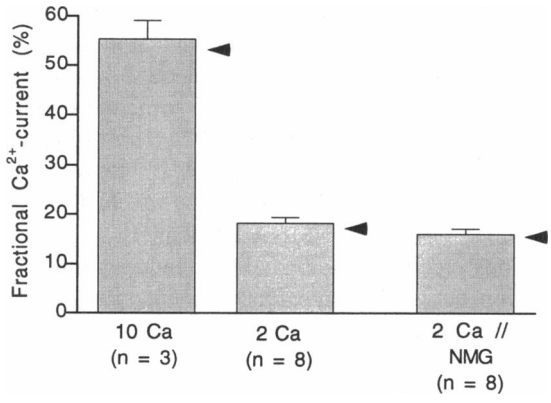

FIGURE 5 Summary of fractional Ca^{2+} currents through NMDA-R channels composed of the NR1-NR2A subunit combination under different ionic conditions. The two leftmost bars represent P_f in the presence of internal permeant cations at 10 or 2 mM $[Ca]_o$ (see Figs. 2 and 3), whereas the right bar refers to the measurements in the absence of internal permeant cations at 2 mM $[Ca]_o$ (Fig. 4). All measurements were made at $V_h = -50$ mV and at 155 mM $[Na]_o$. The predictions of the one-site, two-barrier model (with $P_{Ca}/P_M = 3.6$; see Materials and methods) are shown as arrowheads.

To determine the fractional Ca^{2+} current through NMDA-R channels composed of the NR1-NR2B subunits, *FQ* ratios were measured at 2 mM $[Ca]_o$, 155 mM $[Na]_o$ with the Cs^+-containing internal solution. However, because of the smaller expression level obtained with this subunit combination, reliable recordings could not be made at membrane potentials close to the reversal potential. Therefore, P_f values were calculated using the reference *FQ* ratio obtained for the NR1-NR2A channels under similar ionic conditions (*FQ* = 8.0 BU/nC; see Table 1). The resulting value of P_f (17.5 ± 2.8%, $V_h = -50$ mV, $n = 6$ cells) was not significantly different from the value for the NMDA-R channels composed of NR1-NR2A subunits.

DISCUSSION

The results show that the percentage of current carried by Ca^{2+} through recombinant NMDA-R channels composed of either NR1-NR2A or NR1-NR2B subunits is on the order of 18% at nearly physiological conditions, that is, at a membrane potential of −50 mV, in the presence of permeant monovalent ions and at 2 mM $[Ca]_o$. The measured P_f values are in good agreement with the value predicted by the GHK equation ($P_f = 16\%$) or by a symmetrical one-site, two-barrier model ($P_f = 17.5\%$), using a permeability ratio P_{Ca}/P_M of 3.6, which was obtained from measurements of reversal potential shifts.

Methodological considerations

For calculating the P_f values at 2 and at 10 mM $[Ca]_o$ in the presence of internal and external monovalent permeant ions (see Figs. 2 and 3), it was assumed that $P_f = 100\%$ at $V_{0,M}$, as is predicted by the GHK equations and by a one-site, two-barrier model for ion permeation. This assumption is justified by the finding that the FQ ratios measured at $V_{0,M}$ are similar at three different $[Ca]_o$ (see below for further discussion of this point). The calculated P_f values (see Figs. 3 and 5) are in good agreement with the P_f value found by the second approach, in which a pure flux of Ca^{2+} through the NMDA-R channels was used to calibrate the Ca^{2+} influx signals.

The reference FQ ratios found in this study are in good agreement with previously reported values, which were in the range of 8–10 BU/nC (Zhou and Neher, 1993; Schneggenburger et al., 1993; Burnashev et al., 1995; Garaschuk et al., 1996; in all of these studies the same lot of fluorescent beads was used). However, in the present study there was a roughly 1.2-fold difference in the reference FQ ratio between the NMG^+- and the Cs^+-containing internal solutions (see Table 1), and this difference was statistically significant ($p < 0.01$, unpaired t-test). At present, I have no conclusive explanation for this difference. An observation that could be related to this finding is a progressive increase in cell diameter that was observed during many recordings with the NMG^+-containing internal solution, but which was not apparent during recordings with the Cs^+-containing solutions. It is possible that changes in the viscosity of the cytoplasm after cell swelling led to a change in the fluorescence properties of fura-2 (see also Poenie, 1990). Thus, care should be taken when FQ ratios between experiments with different internal solutions are compared.

For accurate measurements of P_f, it seems helpful to obtain an estimation of the reference FQ ratio in every cell from which P_f measurements are made (see also Vernino et al., 1994; Neher, 1995). When channels with a suffiently high Ca^{2+} permeability are studied, this should be possible to do by taking a reference FQ ratio at $V_{0,M}$, if possible at two different $[Ca]_o$ values to check for the "cross-over" of FQ ratios at $V_{0,M}$ (see Fig. 3). Obtaining the reference FQ ratio in every cell has the advantage that a possible loss of fluorescence intensity does not show up in the calculated P_f value. Indeed, there are some possibilities for loss of fluorescence intensity in P_f measurements, such as a partial saturation of the indicator dye with Ca^{2+} or a loss of fluorescence signal from out-of-focus or out-of-field regions of the cell.

Comparison to previous work

The P_f values reported here for recombinant NMDA-R channels composed of the NR1-NR2A and the NR1-NR2B subunits are larger than the initial value reported for NMDA-R channels in neurons of the medial septum (P_f = 6.8% at 1.6 mM $[Ca]_o$; Schneggenburger et al., 1993), and they are also larger than the P_f value reported recently for NR1-NR2A channels expressed in HEK cells ($P_f = 11\%$ at 1.8 mM $[Ca]_o$; Burnashev et al., 1995). In these two papers, it was hypothesized that the fractional Ca^{2+} current through NMDA-R channels is smaller than predicted by relative permeabilties (P_{Ca}/P_M) using the GHK current equation, a hypothesis that could not be confirmed in the present study.

The reasons for the difference in the measured P_f values between this and the previous studies on neurons in brain slices are probably of methodological origin, although other explanations, such as Ca^{2+} influx through NMDA-R channels assembled from subunits imparting a lower Ca^{2+} permeability (NR2C or NR2D; see Burnashev et al., 1995), cannot be entirely excluded at present. A technical problem of P_f measurements in neurons is the possible loss of fluorescent light from out-of-field or out-of-focus neurites. It should be possible to minimize this problem by using Ca^{2+}-imaging techniques to capture fluorescent light also from fine dendritic processes. With this approach a P_f value of 11% (at 1.6 mM $[Ca]_o$, $V_m = -60$ mV) has been reported recently for NMDA-R channels located on the soma and the proximal part of the apical dendrite of CA1 neurons in hippocampal slices (Garaschuk et al., 1996). Another group (Rogers and Dani, 1995) reported a P_f value of 14.3% (at 2.5 mM $[Ca]_o$, $V_m = -50$ mV) through NMDA-R channels in isolated hippocampal neurons. These values are in closer agreement with the values reported here for recombinant NMDA-R channels.

Implications for ion permeation models

FQ ratios at three $[Ca]_o$ values (2, 5, and 10 mM) crossed over at a membrane potential close (within about ±0.3 mV) to the calculated reversal potential of the monovalent current component ($V_{0,M}$) (see Fig. 3 and Table 1). This is good evidence that the reversal potential of the monovalent current component, which was estimated at low $[Ca]_o$ (0.1 mM), does not change when external Ca^{2+} is added to the bath solution, as is predicted by the principle of independence of ionic movement (Hille, 1992). This argues against a strong coupling between Na^+ and Ca^{2+} fluxes, an effect that would be expected to influence the reversal potential of monovalent ions in the NMDA-R channels.

Previous electrophysiological evidence against a strong interaction between permeating ions includes the finding that the reduction of single-channel conductance by external Ca^{2+} in neuronal NMDA-R channels is monotonic over a wide range of mole fractions of Ca^{2+} and Na^+ (Ascher and Nowak, 1988; Jahr and Stevens, 1993), and the observation of Zarei and Dani (1994) that anomolous mole fraction effects were absent when reversal potentials were measured in mixtures of two permeant ion species. Zarei and Dani (1994) concluded that the NMDA-R channel behaves like a one-ion channel, i.e., that it binds only one permeant ion at a given time. The findings of the present study are compatible with this interpretation. The simplest case of a one-ion

channel model, i.e., a one-site, two-barrier model, was used here to simulate fractional Ca^{2+} currents and provided a reasonable fit of the data (see Fig. 3).

One explanation for the reduction of the NMDA single-channel amplitude by extracellular Ca^{2+} (Ascher and Nowak, 1988; Jahr and Stevens, 1993) assumes that Ca^{2+} binds with a higher affinity than monovalent ions to the site within the channel, which slows the permeation process (see also Nakazawa and Hess, 1993, for the case of ATP-gated ion channels). It is important to note that in a barrier model the predicted P_f values are independent of the well depths and of the absolute barrier heights. Therefore, the affinity of Ca^{2+} binding at a constant P_{Ca}/P_M will not modify the *fractional* contribution of Ca^{2+} to the net inward current, even though the *absolute* amount of Ca^{2+} flowing through the channel will depend on this parameter.

Within the voltage range investigated here, fractional Ca^{2+} currents were in reasonable agreement with the values predicted by the GHK equations. This does not mean that the assumptions made in deriving the GHK equations are all valid. Indeed, a good fit of the data was also obtained with a simple one-site, two-barrier model, provided that the difference in barrier height for monovalent ions and Ca^{2+} was the same for the two barriers. This suggests that the permeation of monovalent ions and Ca^{2+} through NMDA-R channels operates close to the constant offset energy peak condition. Interestingly, it should be possible to test this hypothesis by site-directed mutagenesis. Single point mutations that lead to a reduction of the permeability ratio P_{Ca}/P_M are expected to produce significant deviations of P_f from the GHK-like behavior at negative potentials, if they selectively influence either the inner or the outer energy barrier(s) limiting the access to the permeant ion-binding site.

I am grateful to Dr. Philippe Ascher, in whose laboratory this work was done, for enthusiastic support and for many helpful discussions. I would like to thank Dr. J. Neyton for the subcloning of cDNA clones, Dr. J. Kupper for showing me the transfection protocols, and Drs. B. Barbour and E. Neher for helpful comments on the manuscript.

This work was supported by the CNRS (URA 1857), by the European Union (B1O2-CT93-0243), and by a postdoctoral fellowship to RS (HCM programme, ERBCHB-CT94-1604).

REFERENCES

Ascher, P., and L. Nowak. 1988. The role of divalent cations in the *N*-methyl-D-aspartate responses of mouse central neurones in culture. *J. Physiol.* 399:247–266.

Bliss, T. V. P., and G. L. Collingridge. 1993. A synaptic model of memory: long-term potentiation in the hippocampus. *Nature.* 361:31–39.

Burnashev, N., R. Schoepfer, H. Monyer, J. P. Ruppersberg, W. Günther, P. H. Seeburg, and B. Sakmann. 1992. Control by asparagine residues of calcium permeability and magnesium blockade in the NMDA receptor. *Science.* 257:1415–1419.

Burnashev, N., Z. Zhou, E. Neher, and B. Sakmann. 1995. Fractional calcium currents through recombinant GluR channels of the NMDA, AMPA and kainate receptor subtypes. *J. Physiol.* 485:403–418.

Garaschuk, O., R. Schneggenburger, C. Schirra, F. Tempia, and A. Konnerth. 1996. Fractional calcium currents through somatic and dendritic glutamate receptor channels of hippocampal CA1 pyramidal neurones. *J. Physiol.* 491:757–772.

Grynkiewicz, G., M. Poenie, and R. Y. Tsien. 1985. A new generation of Ca^{2+} indicators with greatly improved fluorescence properties. *J. Biol. Chem.* 260:3440–3450.

Hamill, O. P., A. Marty, E. Neher, B. Sakmann, and F. J. Sigworth. 1981. Improved patch-clamp techniques for high-resolution current recording from cells and cell-free membrane patches. *Pflügers Arch.* 393: 254–261.

Hille, B. 1992. Ionic Channels of Excitable Membranes. Sinauer, Sunderland, MA.

Hollmann, M., J. Boulter, C. Maron, L. Beasley, J. Sullivan, G. Pecht, and S. Heinemann. 1993. Zinc potentiates agonist-induced currents at certain splice variants of the NMDA receptor. *Neuron.* 10:943–954.

Iino, M., S. Ozawa, and K. Tsuzuki. 1990. Permeation of calcium through excitatory amino acid receptor channels in cultured rat hippocampal neurones. *J. Physiol.* 424:151–165.

Jahr, C. E., and C. F. Stevens. 1993. Calcium permeability of the *N*-methyl-D-aspartate receptor channel in hippocampal neurons in culture. *Proc. Natl. Acad. Sci. USA.* 90:11573–11577.

Jan, L. Y., and Y. N. Jan. 1976. L-Glutamate as an excitatory transmitter at the *Drosophila* neuromuscular junction. *J. Physiol.* 262:215–236.

Koh, D. S., J. R. P. Geiger, P. Jonas, and B. Sakmann. 1995. Ca^{2+}-permeable AMPA and NMDA receptor channels in basket cells of rat hippocampal dentate gyrus. *J. Physiol.* 485:383–402.

Konnerth, A., H. D. Lux, and M. Morad. 1987. Proton-induced transformation of calcium channel in chick dorsal root ganglion cells. *J. Physiol.* 386:603–633.

Lewis, C. A. 1979. Ion-concentration dependence of the reversal potential and the single channel conductance of ion channels at the frog neuromuscular junction. *J. Physiol.* 286:417–455.

Lewis, C. A., and C. F. Stevens. 1979. Mechanism of ion permeation through channels in a postsynaptic membrane. *In* Membrane Transport Processes. C. F. Stevens and R. W. Tsien, editors. Raven Press, New York. 133–151.

Lin, F., and C. F. Stevens. 1994. Both open and closed NMDA receptor channels desensitize. *J. Neurosci.* 14:2153–2160.

MacDermott, A. B., M. L. Mayer, G. L. Westbrook, S. L. Smith, and J. L. Barker. 1986. NMDA-receptor activation increases cytoplasmic calcium concentration in cultured spinal cord neurones. *Nature.* 321:519–522.

Malenka, R. C., and R. A. Nicoll. 1993. NMDA-receptor-dependent synaptic plasticity: multiple forms and mechanisms. *Trends Neurosci.* 16: 521–527.

Marshall, J., R. Molloy, G. W. J. Moss, J. R. Howe, and T. E. Hughes. 1995. The jellyfish green fluorescent protein: a new tool for studying ion channel expression and function. *Neuron.* 14:211–215.

Mayer, M. L., A. B. MacDermott, G. L. Westbrook, S. J. Smith, and J. L. Barker. 1987. Agonist and voltage-gated calcium entry in cultured mouse spinal neurons under voltage clamp measured using arsenozo III. *J. Neurosci.* 7:3230–3244.

Mayer, M. L., and G. L. Westbrook. 1987. Permeation and block of *N*-methyl-D-aspartatic acid receptor channels by divalent cations in mouse cultured central neurones. *J. Physiol.* 394:501–527.

Monyer, H., N. Burnashev, D. J. Laurie, B. Sakmann, and P. H. Seeburg. 1994. Developmental and regional expression in the rat brain and functional properties of four NMDA receptors. *Neuron.* 12:529–540.

Monyer, H., R. Sprengel, R. Schoepfer, A. Herb, M. Higuchi, H. Lomeli, N. Burnashev, B. Sakmann, and P. H. Seeburg. 1992. Heteromeric NMDA receptors: molecular and functional distinction of subtypes. *Science.* 256:1217–1221.

Moriyoshi, K., M. Masu, T. Ishii, R. Shigemoto, N. Mizuno, and S. Nakanishi. 1991. Molecular cloning and characterization of the rat NMDA receptor. *Nature.* 354:31–37.

Nakazawa, K., and P. Hess. 1993. Block by calcium of ATP-activated channels in pheochromocytoma cells. *J. Gen. Physiol.* 101:377–392.

Neher, E. 1992. Correction for liquid junction potentials in patch clamp experiments. *Methods Enzymol.* 207:123–131.

Neher, E. 1995. The use of fura-2 for estimating Ca buffers and Ca fluxes. *Neuropharmacology.* 34:1423–1442.

Neher, E., and G. J. Augustine. 1992. Calcium gradients and buffers in bovine chromaffin cells. *J. Physiol.* 450:273–301.

Poenie, M. 1990. Alterations of intracellular fura-2 fluorescence by viscosity: a simple correction. *Cell Calcium.* 11:85–91.

Rogers, M., and J. A. Dani. 1995. Comparison of quantitative calcium flux through NMDA, ATP, and ACh receptor channels. *Biophys. J.* 68: 501–506.

Ruppersberg, J. P., E. v. Kitzing, and R. Schoepfer. 1994. The mechanism of magnesium block of NMDA receptors. *Neurosciences.* 6:87–96.

Schneggenburger, R., Z. Zhou, A. Konnerth, and E. Neher. 1993. Fractional contribution of calcium to the cation current through glutamate receptor channels. *Neuron.* 11:133–143.

Spruston, N., P. Jonas, and B. Sakmann. 1995. Dendritic glutamate receptor channels in rat hippocampal CA3 and CA1 pyramidal neurones. *J. Physiol.* 482:325–352.

Vernino S., M. Rogers, K. A. Radcliffe, and J. A. Dani. 1994. Quantitative measurement of calcium fluxes through muscle and neuronal nicotinic acetylcholine receptors. *J. Neurosci.* 14:5514–5524.

Villaroel, A., N. Burnashev, and B. Sakmann. 1995. Dimensions of the narrow portion of a recombinant NMDA receptor channel. *Biophys. J.* 68:866–875.

Watanabe, M., Y. Inoue, K. Sakimura, and M. Mishina. 1992. Developmental changes in distribution of NMDA receptor channel subunit mRNAs. *Neuroreport.* 3:1138–1140.

Zarei, M. M., and J. A. Dani. 1994. Ionic permeability characteristics of the *N*-methyl-D-aspartate receptor channel. *J. Gen. Physiol.* 103:231–248.

Zhou, Z., and E. Neher. 1993. Calcium permeability of the nicotinic-acetylcholine receptor channels in bovine chromaffin cells. *Pflügers Arch.* 425:511–517.